Fibrinolysis in LPS-induced chronic airway disease

Jordan D. Savov, David M. Brass, Katherine G. Berman, Erin McElvania and David A. Schwartz

Am J Physiol Lung Cell Mol Physiol 285:940-948, 2003. First published Jun 20, 2003;
doi:10.1152/ajplung.00102.2003

Am J Physiol Lung Cell Mol Physiol 285: L940–L948, 2003.
First published June 20, 2003; 10.1152/ajplung.00102.2003.

Fibrinolysis in LPS-induced chronic airway disease

Jordan D. Savov, David M. Brass, Katherine G. Berman, Erin McElvania, and David A. Schwartz

Division of Pulmonary, Allergy, and Critical Care Medicine, Department of Medicine, Duke University Medical Center and Veterans Administration Medical Center, Durham, North Carolina 27710

Submitted 7 April 2003; accepted in final form 20 June 2003

Savov, Jordan D., David M. Brass, Katherine G. Berman, Erin McElvania, and David A. Schwartz. Fibrinolysis in LPS-induced chronic airway disease. *Am J Physiol Lung Cell Mol Physiol* 285: L940–L948, 2003. First published June 20, 2003; 10.1152/ajplung.00102.2003.—To examine the role of the fibrinolytic system in LPS-induced airway disease, we compared the effect of a chronic LPS challenge in plasminogen activator inhibitor-deficient (C57BL/6J$^{PAI\text{-}1-/-}$) mice and wild-type (WT) C57BL/6J mice. Physiological and biological assessments were performed, immediately after, and 4 wk after an 8-wk exposure to LPS or saline. Immediately after the LPS exposure, WT mice had increased estimates of airway reactivity to methacholine compared with C57BL/6J$^{PAI\text{-}1-/-}$ mice; however, airway inflammation was similar in both LPS-exposed groups. Significant increases in both active transforming growth factor (TGF)-β1 and active matrix metalloproteinase (MMP)-9 was detected after LPS exposure in WT but not C57BL/6J$^{PAI\text{-}1-/-}$ mice. C57BL/6J$^{PAI\text{-}1-/-}$ mice showed significantly less TGF-β1 in the lavage and higher MMP-9 in the lung tissue than WT mice at the end of exposure and 4 wk later. After LPS exposure, both WT and C57BL/6J$^{PAI\text{-}1-/-}$ mice had substantial expansion of the subepithelial area of the medium [diameter (d) = 90–129 μm]- and large (d > 129 μm)-size airways when compared with saline-exposed mice. Subepithelial fibrin deposition was prevalent in WT mice but diminished in C57BL/6J$^{PAI\text{-}1-/-}$. PAI-1 expression by nonciliated bronchial epithelial cells was enhanced in LPS-exposed WT mice compared with the saline-exposed group. Four weeks after LPS inhalation, airway hyperreactivity and the expansion of the subepithelial area in the medium and large airways persisted in WT but not C57BL/6J$^{PAI\text{-}1-/-}$ mice. We conclude that an active fibrinolytic system can substantially alter the development and resolution of the postinflammatory airway remodeling observed after chronic LPS inhalation.

airway remodeling; lung inflammation; transforming growth factor-β1; matrix metalloproteinase-9; plasminogen activator inhibitor

ONE ASPECT OF THE ASTHMATIC AIRWAY that is in need of further attention is the mechanisms that regulate the turnover of the extracellular matrix adjacent to the airway epithelia. Components of the fibrinolytic system are among the various factors that have been implicated in the balance between lung tissue injury and repair, or extracellular matrix (ECM) degradation and synthesis. Plasmin, plasminogen activators (PAs), and their inhibitors (PAIs) are the key molecules of the fibrinolytic cascade. The conversion of plasminogen to plasmin is controlled by two distinct types of PAs, tissue type (tPA) and urokinase type (uPA) (35). Plasmin itself is known to digest fibrin(ogen), lyse several other components of ECM (laminin, fibronectin), and to convert matrix metalloproteinases (MMPs) from their latent to active form (27). Two MMPs, MMP-2 and MMP-9, are known to degrade not only denaturated collagens, but also ECM proteins, including type I and IV collagen, fibronectin, and laminin (1). On the other hand, uPA, being a serine protease, acts synergistically, degrading ECM molecules (6). The action of the PAs is opposed and therefore regulated by inhibitors PAI-1, PAI-2, and PAI-3. PAI-1 inhibits both tPA and uPA and is a member of the serine proteinase inhibitor (serpine) enzyme family. Its physiological roles include inhibition of fibrinolytic activity in thrombi and ECM as well as modulation of cell adhesion and migration (37).

During chronic airway inflammation, tissue ECM components degrade, and later, with the healing process, normal tissue remodeling occurs. As a result of damage and tissue inflammation, enhanced extracellular proteolysis takes place because of a leakage of proteases (like PAs) into the interstitial space. PAs will generate plasmin, which will activate latent MMP and further accelerate degradation of ECM proteins. Imbalance between the activity of the factors that degrade (uPA, plasmin, MMPs) vs. those that inhibit degradation [PAI, tissue inhibitors of MMPs (TIMPs)] of ECM can substantially affect the turnover and therefore lead to accumulation of ECM in the tissue.

The pathology of asthma involves chronic airway inflammation and expansion of the subepithelial ECM that involves type I, III, and V collagen (38). In fact, altered expression of PAI-1 may cause a predisposition for the development of asthma in humans (7, 11) and bleomycin-induced pulmonary fibrosis in the murine model (29). PAI-1-deficient mice are protected against the accumulation of ECM deposition and fibrosis in the lung after bleomycin (16) and hyperoxia (3). Enhanced fibrinolytic potential, because of the absence of PAI-1, attenuates the development of postinflammatory re-

Address for reprint requests and other correspondence: J. D. Savov, Duke Univ. Medical Center, P. O. Box 2629, Durham, NC 27710 (E-mail: jsavov@duke.edu).

The costs of publication of this article were defrayed in part by the payment of page charges. The article must therefore be hereby marked "*advertisement*" in accordance with 18 U.S.C. Section 1734 solely to indicate this fact.

modeling of the vascular wall (30) and glomerulosclerosis (15). In vitro experiments indicate that among the cellular sources of PAI-1 in the lung are the mast cells (12), fibroblasts (24), alveolar macrophages (10), and smooth muscle cells (14). In patients with idiopathic pulmonary fibrosis, PAI-1 levels in bronchoalveolar lavage fluid (BALF) are significantly higher than in normal subjects, and alveolar macrophages and type II alveolar epithelial cells are shown to be its source (23).

We have previously shown that chronic inhalation of either grain dust or endotoxin [lipopolysaccharide (LPS)] causes all of the classic features of asthma-airflow obstruction, reversible airway inflammation, persistent airway hyperreactivity, and airway remodeling (19). Moreover, we have demonstrated that the development of chronic airway disease in mice is dependent on the recruitment of polymorphonuclear cells (PMNs) and is associated with the increased expression of transforming growth factor (TGF)-β1 in the mouse conducting airways (31). In the evolution of this condition two phases could be recognized: an early or direct phase (during and immediately after the exposure), which is induced by the consistent and repetitive presence of the stimulus (LPS) and during which infiltration and activation of neutrophils takes place, and a late or indirect phase (4 wk after the exposure), which is characterized by fibrotic airway remodeling and hyperresponsiveness. To further elucidate the pathophysiology of airway remodeling that occurs as a consequence of chronic inflammation induced by LPS inhalation, we investigated the role of fibrinolysis by studying the response of PAI-1-deficient (C57BL/6J$^{PAI\text{-}1-/-}$) mice.

MATERIALS AND METHODS

Study design. To examine the role of the fibrinolytic system in LPS-induced airway disease, we compared the effect of a chronic LPS challenge in C57BL/6J$^{PAI\text{-}1-/-}$ mice and wild-type (WT) C57BL/6J mice. All the mice were 8 wk old and obtained from Jackson Laboratories (Bar Harbor, ME). Mice in each group were evaluated before the exposure (n = 24 per study group), immediately after the 8-wk exposure (LPS or saline; n = 12 per study group), and 4 wk after the end of exposure (n = 12 per study group). The study protocol was in accordance with guidelines set forth by the Duke University Animal Care and Use Committee.

Endotoxin preparation and LPS aerosol exposures. LPS (*Escherichia coli* serotype 0111:B4 from Sigma, St. Louis, MO) was reconstituted with 10 ml of sterile PBS, and stock aliquots (2.5 mg/ml) were stored at −20°C. Stock aliquots were thawed once and stored at 4°C thereafter. Immediately before use, 0.7 ml of LPS stock (1.75 mg; 2,625,000 EU) was diluted in 100 ml of PBS for nebulization. Mice were placed in individual compartments of stainless steel wire cage exposure racks in two 20-liter chambers with one for LPS exposure and the other for sterile saline exposure. Animals were exposed for 4 h per day, 5 days per wk, over an 8-wk period. Endotoxin solution and pyrogen-free, isotonic saline (Baxter Healthcare, Deerfield, IL) were aerosolized with a constant-output six-jet Collison nebulizer (model CN-25; BGI, Waltham, MA) with all of the output directed into the exposure chamber. Filtered, dehumidified air was supplied to the nebulizer at 20 psi of gauge pressure and at a flow rate of ~3.3 l/min. The chamber was exhausted at a flow rate of 27.0 l/min.

Endotoxin assay. The airborne concentration of endotoxin was assessed by sampling air drawn from the exposure chamber through a 37-mm binder-free glass-fiber filter (Whatman, Mainstone, UK) held within a 47-mm in-line air-sampling filter holder (Gelman model 2220). Filters were placed in pyrogen-free petri dishes with 2 ml of sterile PBS containing 0.05% Tween 20 (Sigma) and then placed on a rotating shaker at room temperature for 1 h. Aliquots of the wash solution were serially diluted in pyrogen-free water and tested for endotoxin using a chromogenic *Limulus* amebocyte lysate assay (QCL-1000; BioWhittaker, Walkersville, MD) according to the manufacturer's instructions. The mean daily endotoxin concentration (EU/m^3) was determined and the mean during the 8-wk exposure period. The corresponding actual concentration was calculated (4.50 ± 0.20 μg/m^3) according to the Sigma certificate of analysis.

Barometric plethysmography. A noninvasive method (whole body plethysmography) was used to estimate respiratory response to methacholine (MCh) aerosol challenge. Four assessments were performed: before the exposure, after first half of the exposure (4 wk), at the end of the exposure (8 wk), and 4 wk after the end of the exposure. Individual mice were placed in 3-in-diameter chambers (Buxco Electronics, Troy, NY) that were ventilated by bias airflow at a rate of 0.5 l·min^{-1}·chamber^{-1}. Airflow obstruction in the mice was induced with a MCh (Sigma) aerosol challenge. In each plethysmograph, a pressure signal was generated from the pressure difference of the main chamber containing the unrestrained mouse and a reference chamber, which cancels atmospheric disturbances. Signals were analyzed to derive whole body respiratory parameters (SFT3812, BioSystem XA version 2.0.2.48, Buxco), including respiratory rate, tidal volume, inspiratory and expiratory times (T_I and T_E, respectively), peak inspiratory and expiratory flows (PIF and PEF, respectively), and relaxation time (T_R). These parameters are used by the program software to calculate enhanced pause (P_{enh}, unitless), using the following expression: $P_{enh} = [(T_E - T_R)/T_R] \times (PEF/PIF)$. P_{enh} has been found to correlate with lung resistance (20) and is associated with changes in pulmonary resistance during bronchoconstriction. Mice were left to acclimatize inside the chambers for 15 min, and then their respiratory responses were evaluated at baseline (saline provoked) and after increasing doses of aerosolized MCh (5, 10, and 20 mg/ml). The different concentrations of aerosolized MCh were administered for 1 min using an ultrasonic nebulizer and nebulizer control unit (Buxco Electronics). During MCh challenge, P_{enh} changes have been demonstrated empirically to correlate with changes in pulmonary resistance and are therefore believed to represent airway obstruction; however, this remains controversial (25). Recording of breathing parameters began immediately after the end of MCh aerosolization and continued for 10 min. Average P_{enh} values were determined over the first 3 min (early phase) of the respiratory response to the MCh aerosol.

Whole lung lavage. Mice were euthanized by CO_2 inhalation, the trachea was then exposed, and the lungs were lavaged through a PE-90 tube with 6.0 ml of sterile saline. The saline was infused 1 ml at a time at an infusion pressure of 25 cmH_2O. Return volume was recorded and was consistently >4.5 ml. Processing of the lavage fluid has been described previously (33). Briefly, the lavage fluid was centrifuged for 5 min at 600 *g*. The supernatant was decanted and stored at −70°C for further use. The cell pellet was resuspended with Hanks' balanced salt solution (without Ca or Mg) and washed twice. A small aliquot of resuspended

cells was used for counting total number of cells using a Bright-Line hemocytometer (Hausser Scientific, Horsham, PA). The cell suspension (75–100 μl) from each probe was spun onto a positively charged glass slide using a Shandon Cytospin centrifuge (Shandon, Southern Sewickley, PA). Postcytospin, cells were stained with HEMA-3 stain, air-dried, and covered with a coverslip with Cytoseal (Stephens Scientific, Kalamazoo, MI). Differential counts of lavage cells were performed at ×400 (dry objective) under an Olympus microscope (Olympus). Two hundred random cells were counted from each slide.

Lung lavage TGF-β1 assay. The lavage supernatant was stored at −70°C. The levels of TGF-β1 in lung lavage fluid were measured by a sandwich enzyme-linked immunosorbent assay, using a mouse kit (Promega, Madison, WI). Active and total TGF-β1 in the lavage supernatant was assessed following the manufacturer's instructions.

Assay for detection of MMP-9. The level of active MMP-9 in the lung tissue homogenates was determined with the chromogenic assay (Amersham Biosciences, Piscataway, NJ) according to manufacturer's instructions. In brief, the active MMP-9 in tissue sample supernatant cleaved a modified prourokinase, and the activity of generated urokinase was measured through cleavage of a chromogenic peptide. The resulting color was read at 405 nm. The lower limit of detection of the assay was 1.5 pg/ml.

Tissue preparation. Lungs were perfused with 0.9% saline through the pulmonary artery to remove blood from the vascular bed. The whole right lung was removed and snap-frozen in liquid nitrogen and stored at −70°C for later use. Freshly prepared ice-cold 4% paraformaldehyde (Fisher Scientific, Pittsburgh, PA) in 1× PBS (pH 7.4) was instilled through the tracheal cannula at a constant pressure of 25 cmH_2O to inflate fix the left lung. Specimens (that consist of the whole single-lobed left lung) were immersed in 4% paraformaldehyde at 4°C overnight and dehydrated in a graded series of ethanol solutions. Tissue was embedded in paraffin, and sections were cut at 5-μm thickness for evaluation.

Morphometric analysis. Morphometric measurements of cross-sectional areas were performed in a blinded manner on transverse bronchial sections (Masson Trichrome stained) using a computer-assisted image analysis system, as described previously (31). Measurements were performed on sections obtained from equivalent positions (80 μm apart) along the tissue blocks. Briefly, internal airway perimeter, external airway perimeter, and basement membrane perimeter were outlined and measured at ×200 magnification. The area of airway subepithelial tissue was calculated with these measurements. On the basis of the airway lumen diameter, all airway profiles were divided into three representative groups, i.e., small (≤90 μm), medium (>90–129 μm), and large (>129 μm) (19). For every profile, the subepithelial area was normalized to the length of the adjacent basal membrane. The measurements from four sections per animal in all the groups were then averaged per animal. Data are reported as group mean ± SE for each airway size of these average values obtained in all animals analyzed.

Immunohistochemical analysis. For fibrin(ogen) immunostaining, sections underwent high temperature and pressure antigen-unmasking procedure with citrate buffer, pH 6.0 (Zymed Laboratories, South San Francisco, CA), followed by endogenous peroxidase blocking with 0.3% H_2O_2 for 30 min at room temperature and a rinse in blocking normal rabbit serum. The sections were then incubated in a goat anti-mouse fibrin(ogen) antibody (Nordic Immunology, Tillburg, The Netherlands), followed by the biotinylated secondary antibody (rabbit anti-goat IgG), and the avidin-biotin complex (ABC) reagent from Vectastain ABC Kit (Vector Laboratories, Burlingame, CA). Peroxidase activity was detected with 3,3′-diaminobenzidine (Vector Laboratories) and H_2O_2, after which a light counterstain with hematoxylin was performed.

Immunohistochemical identification of PAI-1-positive cell types was accomplished using a rabbit anti-mouse PAI-1 polyclonal antibody (Molecular Innovations, Southfield, MI). After blocking endogenous peroxidase, the slides were incubated either with active antibody (1:300) or with normal rabbit IgG as a negative control. The secondary antibody was biotin-conjugated goat anti-rabbit IgG (Vector Laboratories), which was followed by standard avidin-biotin horseradish peroxidase reaction (ABC technique). Peroxidase activity detection and counterstaining were performed as described above.

Statistical analyses. All data are expressed as means ± SE. We primarily compared the physiological and biological (BALF cellularity and airway morphometry) responses in C57BL/6J$^{PAI\text{-}1-/-}$ and WT mice following an 8-wk exposure and again following a 4-wk recovery. The difference between the two variables was analyzed by the Mann-Whitney *U*-test (18). Probability values of $P < 0.05$ (two-tailed) were considered statistically significant.

RESULTS

Airway physiology. The whole body plethysmography was performed before the exposure, after 4 wk of LPS or saline inhalation, at the end of the exposure (8 wk), and 4 wk after the end of the exposure. The maximum responses to MCh (expressed as P_{enh}) were observed at the highest dose of MCh (20 mg/ml). Before the exposure, no differences were observed between the WT and C57BL/6J$^{PAI\text{-}1-/-}$ respiratory response (data not shown). After a 4-wk exposure, LPS-exposed WT mice showed significantly increased P_{enh} values in response to 10 and 20 mg/ml MCh compared with LPS-exposed C57BL/6J$^{PAI\text{-}1-/-}$ mice (Fig. 1), whereas saline-exposed mice from both groups showed no change from preexposure values. At the end of the 8-wk exposure period, LPS-exposed WT mice demonstrated significant increases in respiratory response compared with LPS-exposed C57BL/6J$^{PAI\text{-}1-/-}$ mice, however, only after inhaling 20 mg/ml MCh (Fig. 1). After a 4-wk recovery, LPS-exposed C57BL/6J$^{PAI\text{-}1-/-}$ mice presented a level of respiratory response to MCh negligibly different (4–6% higher) from saline-exposed age-matched controls. In contrast, the LPS-exposed WT group demonstrated more pronounced enhancement in airway responsiveness to MCh, which was significant compared with the LPS-exposed C57BL/6J$^{PAI\text{-}1-/-}$ mice.

Whole lung lavage cellularity. After 8 wk of LPS exposure, WT and C57BL/6J$^{PAI\text{-}1-/-}$ mice demonstrated substantial increases in the total number of the lavage cells compared with saline-exposed groups, with PMNs the predominant cell type (Table 1). Four weeks after the exposure, the lavage fluid total cell concentration of the LPS-exposed groups had returned to levels compatible with those of saline-exposed age-matched controls, and the cells were predominately macrophages.

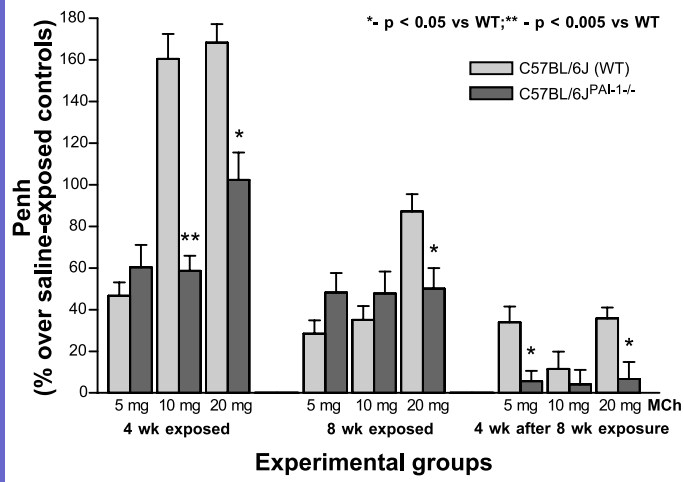

Fig. 1. Barometric plethysmography measures of LPS-induced airway hyperresponsiveness to inhaled methacholine (MCh). Mean values (± SE) of enhanced pause (Penh), expressed as a percentage above saline-exposed age-matched controls, are shown for LPS-exposed mouse groups after 4-wk LPS exposure (n = 12 in each group), after 8-wk LPS exposure (n = 12 in each group), and 4 wk after an 8-wk LPS exposure (n = 6 in each group). Significant difference within the LPS-exposed group [**$P < 0.005$; *$P < 0.05$ plasminogen activator inhibitor-deficient (C57BL/6J$^{PAI-1-/-}$) vs. wild-type (WT) C57BL/6J mice].

Lung lavage TGF-β1. After the 8-wk exposure to LPS, the total TGF-β1 in lavage fluid of WT mice was found to be significantly ($P < 0.05$) greater compared with the levels that was observed in the C57BL/6J$^{PAI-1-/-}$ mice; however, the percent increase above free air-exposed mice was no different between these two strains (Fig. 2*A*). Similar patterns were observed for the active TGF-β1 profiles (Fig. 2*B*), but the increase in the level of the active form of the molecule determined in WT, LPS-exposed mice compared with WT, saline-exposed mice was significant ($P < 0.05$). Not only were the absolute mean values significantly different, but the mean percentage of the active form (based on the total TGF-β1 content) also showed significant increase in WT, LPS-challenged mice (80% in LPS-exposed vs. 51% in saline-exposed controls). In contrast, among C57BL/6J$^{PAI-1-/-}$ mice, no significant difference was observed in lavage concentration of TGF-β1 following inhalation of LPS. After 4 wk of recovery from the exposure, the significant differences between WT and C57BL/6J$^{PAI-1-/-}$ mice in levels of lavage TGF-β1 (total and active) persisted. In fact, while WT mice continued to demonstrate a substantial percent increase in total and active TGF-β1, C57BL/6J$^{PAI-1-/-}$ mice had a trivial increase in these measures after the recovery period.

Histopathology. Lung tissue sections at the end of the 8-wk exposure demonstrated an increase in inflammatory cell infiltration in LPS-exposed WT and C57BL/6J$^{PAI-1-/-}$ mice. Stereological measurements performed using Masson Trichrome stains reveal that the subepithelial compartment was significantly ($P < 0.005$) expanded in size in small, medium, and large airways from WT LPS-exposed mice relative to same-size airways from WT saline-exposed mice (Fig. 3*A*). Similarly, among C57BL/6J$^{PAI-1-/-}$ mice, expansion of the subepithelial region was observed in the medium ($P < 0.005$) and large ($P < 0.05$) airways (Fig. 3*A*). The wall enlargement in the WT LPS-exposed group consisted primarily of PMNs together with significant fibrin deposits as demonstrated immunohistochemically (Fig. 4). This was in contrast to the appearance of the inflammatory lesion observed in C57BL/6J$^{PAI-1-/-}$ LPS-exposed mice, wherein there were infiltrating PMNs, but no fibrin was observed (Fig. 4). There was no significant difference in the degree of subepithelial expansion between WT and C57BL/6J$^{PAI-1-/-}$ LPS-exposed mice immediately after the 8-wk exposure.

After the 4-wk recovery period, lung sections from WT LPS-exposed mice revealed expansion of the subepithelial region of medium- and large-size airways compared with the same-size airways from WT saline-exposed controls (Fig. 3*B*). Those thickened airway walls showed scattered inflammatory cells in the subepithelial tissue zone, did not stain positive for fibrin (Fig. 4), but demonstrated enhanced collagen deposition on Masson Trichrome stains. The subepithelial region of the large-size airways in WT LPS-exposed mice was also significantly larger than observed in the same compartment in C57BL/6J$^{PAI-1-/-}$ LPS-exposed mice at this time point (Fig. 3*B*). Moreover, 4 wk following the exposure to LPS, compared with the saline-exposed controls, the C57BL/6J$^{PAI-1-/-}$ mice no longer demonstrated expansion of the subepithelial region.

Immunohistological analysis. Chronic inhalation of LPS enhanced the expression of PAI-1 in WT mice (Fig. 5). Within the airway epithelia, nonciliated bronchial

Table 1. *Lung lavage cellularity immediately and 4 wk after an 8-wk inhalation exposure to saline or LPS*

	Immediately After Exposure				4 Wk After Exposure			
Cells (×10^3/ml)	WT (saline)	C57BL/6J$^{PAI-1-/-}$ (saline)	WT (LPS)	C57BL/6J$^{PAI-1-/-}$ (LPS)	WT (saline)	C57BL/6J$^{PAI-1-/-}$ (saline)	WT (LPS)	C57BL/6J$^{PAI-1-/-}$ (LPS)
Total cells	13.3 ± 4.1	18.9 ± 3.8	157.1 ± 5.4	141.7 ± 13.1	23.4 ± 2.0	28.4 ± 3.4	30.6 ± 5.1	28.3 ± 5.4
Macrophages	13.8 ± 2.0	17.0 ± 1.8	25.4 ± 2.3	27.7 ± 3.9	22.1 ± 1.9	24.9 ± 2.4	27.5 ± 4.6	24.4 ± 4.1
Neutrophils	0 ± 0	0.2 ± 0.1	118.7 ± 7.5	103.9 ± 9.5	0.1 ± 0.1	0.5 ± 0.3	0 ± 0	0 ± 0
Lymphocytes	0.2 ± 0.1	0.4 ± 0.1	12.5 ± 2.9	11.9 ± 2.5	0.7 ± 0.2	1.3 ± 0.3	2.0 ± 0.5	2.0 ± 0.8
Airway epithelial	0.3 ± 0.1	0.5 ± 0.1	0.5 ± 0.5	2.2 ± 1.0	1.0 ± 0.3	1.3 ± 0.2	1.0 ± 0.2	1.9 ± 0.7

Values are means ± SE for n = 6 in each group. LPS causes a similar pattern and magnitude of inflammatory cell recruitment in wild-type (WT) and plasminogen activator inhibitor-deficient (C57BL/6J$^{PAI-1-/-}$) mice. Saline-exposed controls (at both time points) show similar numbers.

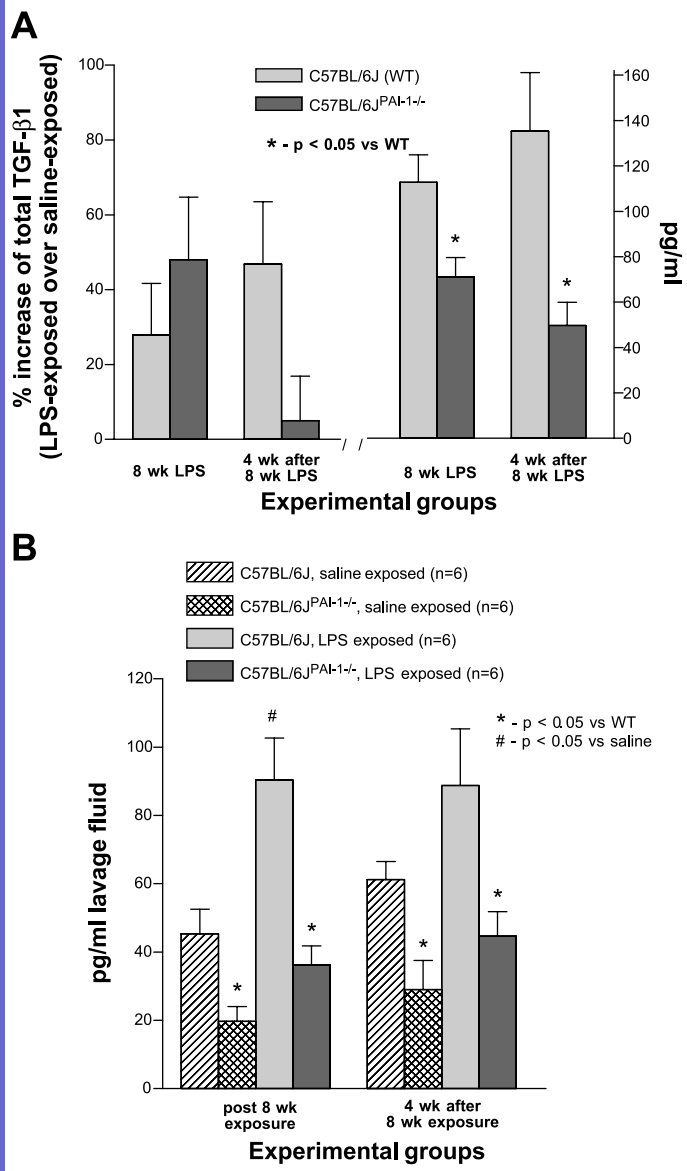

Fig. 2. Transforming growth factor (TGF)-β1 concentration in the lavage fluid. *A*: total TGF-β1 immediately after and 4 wk following an 8-wk LPS exposure. Data are presented as a percentage over saline-exposed groups and as means ± SE values (pg/ml). *B*: active TGF-β1 (pg/ml) at the end of an 8-wk exposure and after 4-wk recovery. C57BL/6J$^{PAI-1-/-}$ group is showing significantly (*P < 0.05) lower level of active and total TGF-β1 at both time points; #P < 0.05 vs. the corresponding saline-exposed group of mice.

cells (Clara cells) were found to be PAI-1 positive, whereas ciliated cells were PAI-1 negative. This was most evident in the smaller airways that were completely lined by nonciliated cells and stained uniformly positive for PAI-1. In the subepithelial region, single cells, part of the inflammatory infiltrates, were also positively stained for PAI-1. After the 4-wk recovery period, WT mice that had been exposed to LPS showed sustained expression of PAI-1 in nonciliated bronchial epithelial cells (Fig. 5).

MMP-9 activity in lung tissue homogenates. Among C57BL/6J$^{PAI-1-/-}$ mice, high levels of MMP-9 activity were observed in the lung tissue after an 8-wk exposure to either saline or LPS, but no difference was observed in MMP-9 activity between these two exposures (Fig. 6). In contrast, among WT mice, LPS exposure resulted in elevation of the amount of active MMP-9 in the lung tissue when compared with saline exposed. However, even among LPS-exposed WT mice, the level of MMP-9 was significantly less than observed in LPS-exposed C57BL/6J$^{PAI-1-/-}$ mice. After the 4-wk recovery period, the WT groups (saline and LPS exposed) demonstrated negligible amounts of active tissue MMP-9, whereas C57BL/6J$^{PAI-1-/-}$ mice continued to have high concentrations of MMP-9 in the lung tissue.

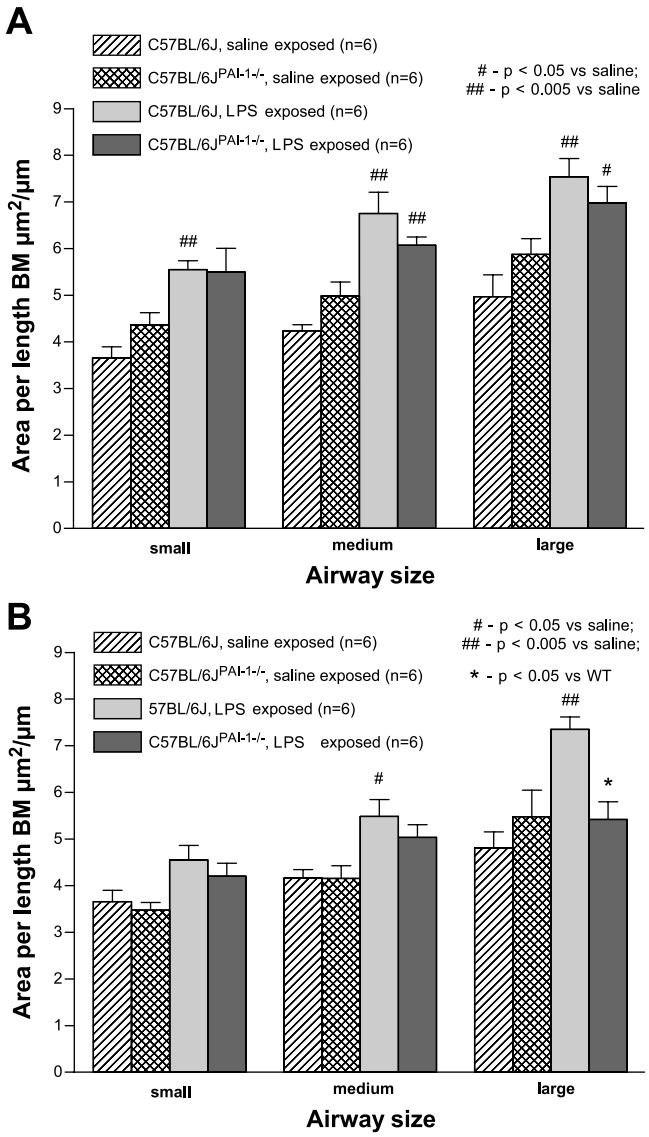

Fig. 3. Values obtained by morphometric analysis for 3 sizes of airways: small (diameter ≤90 μm), medium (>90–129 μm), and large (>129 μm). *A*: subepithelial area per length of basal membrane (BM) after completion of an 8-wk exposure. *B*: normalized measurements for the subepithelial area from recovered group of animals. All values are presented as means ± SE. Significant difference compared with the corresponding saline-exposed controls (#P < 0.05 and ##P < 0.005, respectively); *P < 0.05 vs. the corresponding WT group of mice.

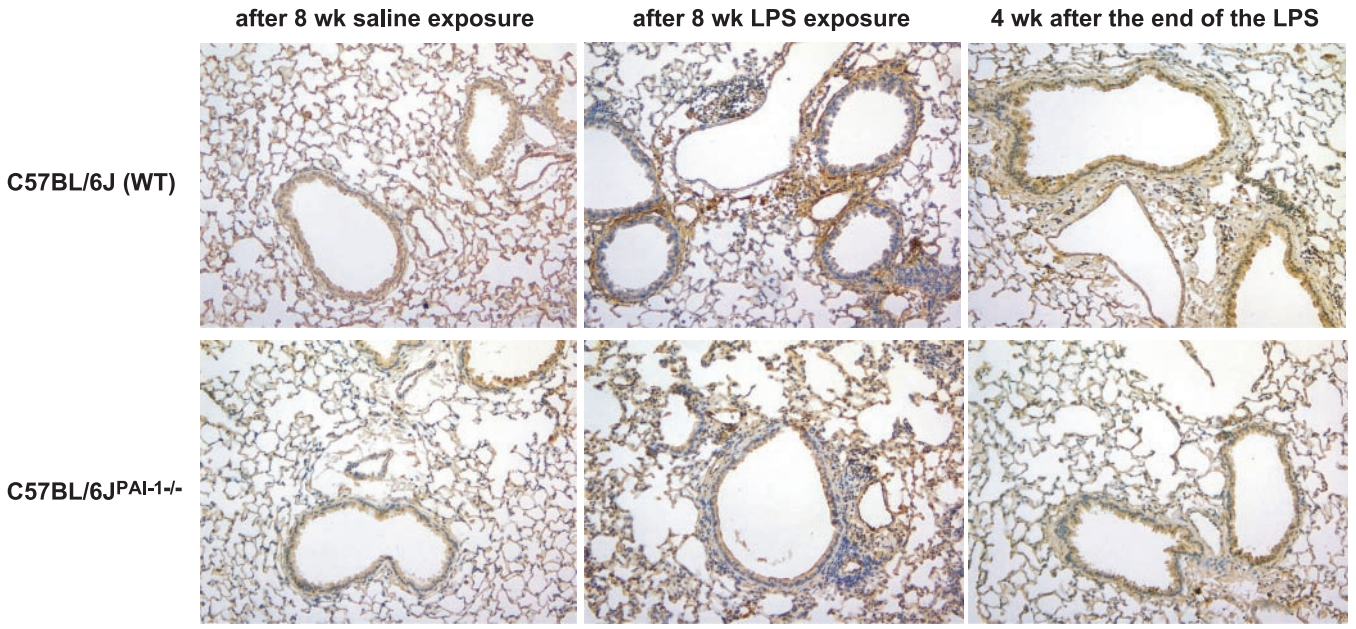

Fig. 4. Immunohistochemistry illustrating fibrin(ogen) deposition. Saline-exposed animals (C57BL/6J WT and C57BL/6J$^{PAI-1-/-}$) show no positive stain. After LPS exposure, airways from a WT animal show fibrin-rich material under the epithelium, whereas an airway profile from a C57BL/6J$^{PAI-1-/-}$ animal displays polymorphonuclear cell-rich but fibrin-poor infiltrate in the airway wall. Four weeks after the completion of an 8-wk LPS-exposure, C57BL/6J mice are showing lack of fibrin immunostain in the thickened airway wall. Positive staining is visualized by a brown color [3,3′-diaminobenzidine (DAB) reaction product]. Original magnification for all photomicrographs, ×200.

DISCUSSION

We conclude that an active fibrinolytic system can substantially alter the development and resolution of the pathological matrix in the airway subepithelium that is observed following chronic inhalation of LPS. Mice deficient in PAI-1 develop PMN-rich but fibrin-poor expansion of airway subepithelial matrix after chronic LPS challenge, were able to resolve the lesion much more quickly than the WT mice, and did not go on to develop persistent airway remodeling.

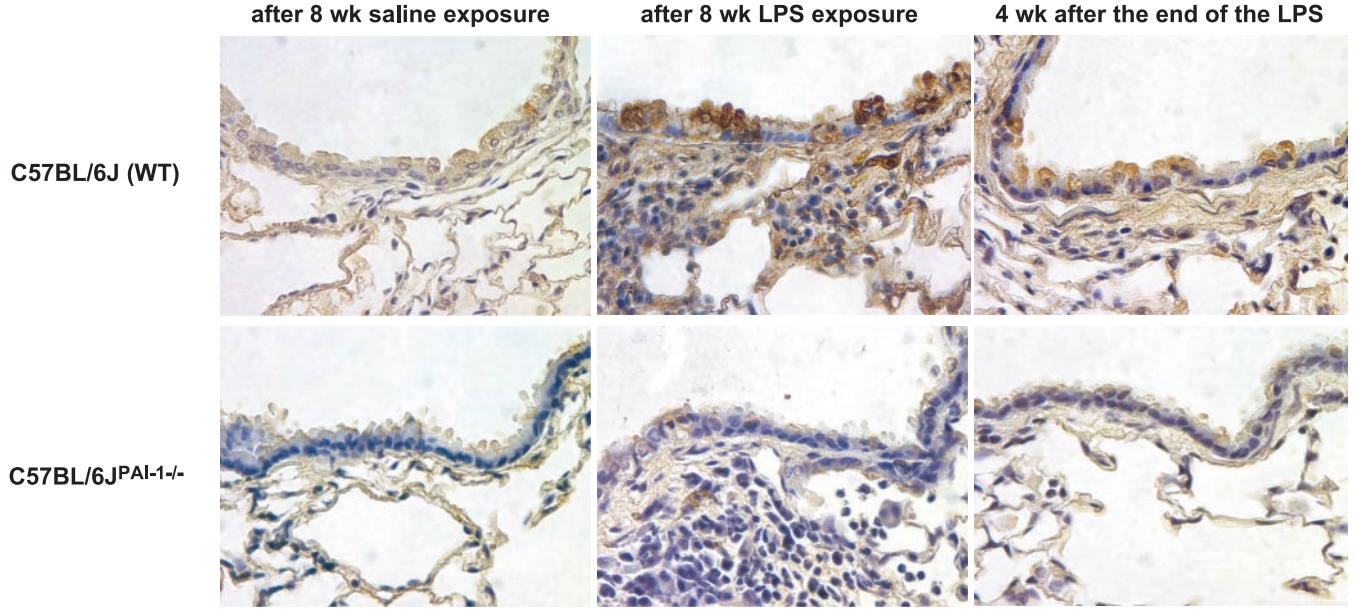

Fig. 5. Plasminogen activator inhibitor (PAI)-1 expression detected by immunohistochemistry. Representative histological lung sections from C57BL/6J (WT) and C57BL/6J$^{PAI-1-/-}$ mice at the end of either saline or LPS exposure and at 4 wk after the completion of an 8-wk LPS exposure. WT animals are showing positive PAI-1 immunostain in nonciliated bronchiolar epithelial cells after LPS exposure and 4 wk later. Positive staining is visualized by a brown color (DAB reaction product). Original magnification for all photomicrographs, ×400.

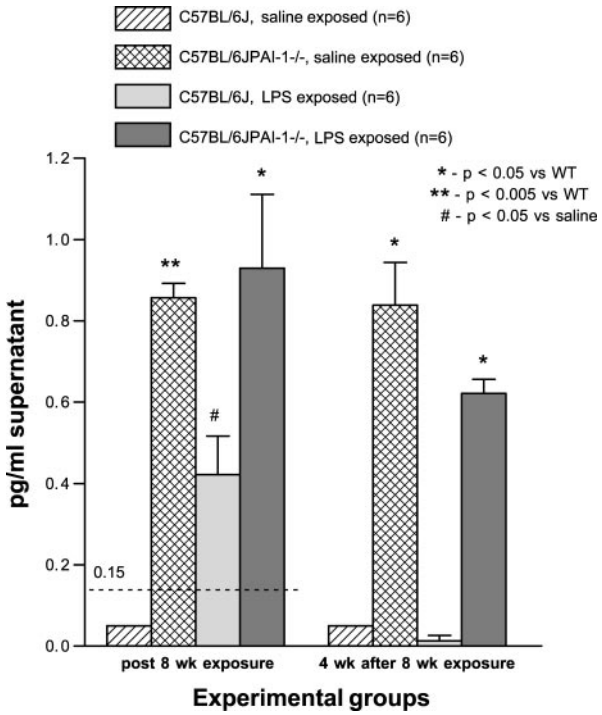

Fig. 6. Levels of active matrix metalloproteinase (MMP)-9 in the supernatants of lung tissue homogenates assessed after 8-wk exposure and 4 wk after the end of 8-wk exposure. MMP-9 activity is significantly elevated in lung tissue from C57BL/6J$^{PAI-1-/-}$ groups compared with WT groups in both time points and both exposure conditions. All values are presented as means ± SE. #$P < 0.05$ vs. the corresponding saline-exposed group of mice.

PAI-1 is an important physiological regulator for the generation of plasmin. The congenital absence of PAI-1, a condition that has been described in humans and generated in mice, produces a phenotype characterized by hyperfibrinolytic state, increased bleeding, and greater resistance to venous thrombosis (8, 9, 35). PAI-1 deficiency limits bleomycin-induced lung interstitial fibrosis through unopposed plasmin generation (34). We found that PAI-1 depletion did not affect the level of LPS-induced neutrophilic inflammation in the lung. The concentration of PMNs in the lavage fluid was equivalently increased in both WT and C57BL/6J$^{PAI-1-/-}$ mice immediately and 4 wk after the exposure to LPS. This suggests that reducing the neutrophilic inflammation was not the mechanism through which PAI-1-deficient mice were protected from development of chronic LPS-induced airway disease. Similar findings were observed for bleomycin (21) in PAI-1-deficient mice.

Endotoxin has been described to be a PAI-1 agonist in vivo and in vitro (17, 32). In this study we were able to demonstrate induction of PAI-1 expression in nonciliated bronchial epithelial cells after chronic LPS inhalation exposure, which might lead to an antifibrinolitic environment within the airway wall with resultant fibrin deposition. PAI-1 deficiency resulted in the development of fibrin-poor inflammatory infiltrates and subsequent full resolution of the airway lesion. Our results suggest that PAI-1 may manifest its effect on postinflammatory ECM remodeling by regulating the extent of the fibrin deposition. Accumulated fibrin within the airway wall may influence lesion evolution by several other potential mechanisms. First, fibrin(ogen) may serve as a key adhesion molecule, promoting the recruitment and local stabilization of inflammatory cells. Fibrin matrices may support the migration and local proliferation of smooth muscle cells (22) or fibroblasts (13). Finally, plasmin-generated fibrin degradation products (FDPs) produced within airway lesions may also be biologically significant in lesion progression. Specific FDPs appear to have both mitogenic and angiogenic activities, properties (28) that may contribute to airway remodeling in vivo.

TGF-β1 is thought to promote net ECM deposition through simultaneous mechanisms: *1*) by increasing fibroblast proliferation and collagen production, *2*) by downregulating protease activity (of the enzymes such as interstitial collagenase), and *3*) by upregulating expression of TIMPs as well as upregulating of PAI-1. In previous experiments, we have found that expression of TGF-β1 in the mouse conducting airways increases after chronic LPS inhalation challenge and is dependent on neutrophilic infiltration and associated with subsequent collagen deposition in the airway subepithelia (31). In this study, we demonstrated that the amount of TGF-β1 in lavage fluid is greater in WT mice than in C57BL/6J$^{PAI-1-/-}$ mice. This difference was not dependent on the inflammatory cell recruitment (the degree of airway inflammation was similar in C57BL/6J$^{PAI-1-/-}$ and WT mice). Not only did C57BL/6J$^{PAI-1-/-}$ mice underexpress TGF-β1, but in contrast to WT mice, C57BL/6J$^{PAI-1-/-}$ mice did not demonstrate an LPS-dependent increase in TGF-β1 levels. These findings suggest that TGF-β1 may serve to enhance the severity of the airway response to inhaled LPS.

Importantly, PAI-1-deficient mice have marked upregulation of MMP-9 in the lung. Being a component of PMN secondary granules, MMP-9 (gelatinase B) is thought to be required for efficient transit of neutrophils from vascular lumen, through subendothelial matrix, and into tissues. However, several recent studies have shown that in the lung, MMP-9 activation is not necessary for the transmigration of neutrophils (2, 4, 26), which is entirely consistent with our findings. Alternatively, active MMP-9 may either proteolytically activate cytokines or accelerate the cleavage of molecules involved in airway fibrosis (36). In fact, MMP-9 and MMP-2 are able to proteolytically degrade TGF-β1 producing different cleavage products, suggesting different recognition sites for the two gelatinases (39). Whether the products of TGF-β1 cleavage will display activity in vivo or will be inactive intermediates is not clear. On the basis of these observations, we speculate that the mechanism by which PAI-1 deficiency influences the fibrotic response in this model involves the enhanced activity of MMP-9 in the lung tissue of PAI-1-deficient mice, which may in turn enzymatically degrade and inactivate TGF-β1. Finally, it has been described that fibrinogen and fibrin themselves are substrates for selected MMPs, which presumes that

certain MMPs might participate in fibrin removal in normal ECM turnover and pathological matrix resolution (5).

Our findings clearly demonstrate that the development of chronic LPS-induced airway disease is associated with fibrin deposition and enhanced expression of PAI-1 in the airways, together with an increased activation of TGF-β1 and enhanced expression of MMP-9. Although C57BL/6J$^{PAI\text{-}1-/-}$ mice develop LPS-induced PMN-rich and fibrin-poor expansion of the airway subepithelial zone during the early phase of the disease, these mice resolve this airway lesion and consequently do not develop the late phase that is characterized by subepithelial fibrosis and persistent airway hyperreactivity. In aggregate, these findings suggest that fibrinolysis is important in resolving the subepithelial expansion and minimizing fibrosis that is typically observed in chronic LPS-induced airway disease. These findings may prove relevant in asthma.

The authors acknowledge the excellent technical assistance of Kristina Riebe. They are especially grateful to Martha Sue Carraway for scientific advice.

DISCLOSURES

This study was supported by grants from the Department of Veterans Administration (Merit Review), the National Institute of Environmental Health Sciences (ES-11375, ES-07498, and ES-09607), and the National Heart Lung and Blood Institute (HL-67467, HL-66611, and HL-66604).

REFERENCES

1. **Aimes RT and Quigley JP.** Matrix metalloproteinase-2 is an interstitial collagenase. Inhibitor-free enzyme catalyzes the cleavage of collagen fibrils and soluble native type I collagen generating the specific 3/4- and 1/4-length fragments. *J Biol Chem* 270: 5872–5876, 1995.
2. **Allport JR, Lim YC, Shipley JM, Senior RM, Shapiro SD, Matsuyoshi N, Vestweber D, and Luscinskas FW.** Neutrophils from MMP-9- or neutrophil elastase-deficient mice show no defect in transendothelial migration under flow in vitro. *J Leukoc Biol* 71: 821–828, 2002.
3. **Barazzone C, Belin D, Piguet PF, Vassalli JD, and Sappino AP.** Plasminogen activator inhibitor-1 in acute hyperoxic mouse lung injury. *J Clin Invest* 98: 2666–2673, 1996.
4. **Betsuyaku T, Shipley JM, Liu Z, and Senior RM.** Neutrophil emigration in the lungs, peritoneum, and skin does not require gelatinase B. *Am J Respir Cell Mol Biol* 20: 1303–1309, 1999.
5. **Bini A, Wu D, Schnuer J, and Kudryk BJ.** Characterization of stromelysin 1 (MMP-3), matrilysin (MMP-7), and membrane type 1 matrix metalloproteinase (MT1-MMP) derived fibrin (ogen) fragments D-dimer and D-like monomer: NH2-terminal sequences of late-stage digest fragments. *Biochemistry* 38: 13928–13936, 1999.
6. **Blasi F, Vassalli JD, and Dano K.** Urokinase-type plasminogen activator: proenzyme, receptor, and inhibitors. *J Cell Biol* 104: 801–804, 1987.
7. **Buckova D, Izakovicova Holla L, and Vacha J.** Polymorphism 4G/5G in the plasminogen activator inhibitor-1 (PAI-1) gene is associated with IgE-mediated allergic diseases and asthma in the Czech population. *Allergy* 57: 446–448, 2002.
8. **Carmeliet P, Kieckens L, Schoonjans L, Ream B, van Nuffelen A, Prendergast G, Cole M, Bronson R, Collen D, and Mulligan RC.** Plasminogen activator inhibitor-1 gene-deficient mice. I. Generation by homologous recombination and characterization. *J Clin Invest* 92: 2746–2755, 1993.
9. **Carmeliet P, Stassen JM, Schoonjans L, Ream B, van den Oord JJ, De Mol M, Mulligan RC, and Collen D.** Plasminogen activator inhibitor-1 gene-deficient mice. II. Effects on hemostasis, thrombosis, and thrombolysis. *J Clin Invest* 92: 2756–2760, 1993.
10. **Chapman HA, Yang XL, Sailor LZ, and Sugarbaker DJ.** Developmental expression of plasminogen activator inhibitor type 1 by human alveolar macrophages. Possible role in lung injury. *J Immunol* 145: 3398–3405, 1990.
11. **Cho SH, Hall IP, Wheatley A, Dewar J, Abraha D, Del Mundo J, Lee H, and Oh CK.** Possible role of the 4G/5G polymorphism of the plasminogen activator inhibitor 1 gene in the development of asthma. *J Allergy Clin Immunol* 108: 212–214, 2001.
12. **Cho SH, Tam SW, Demissie-Sanders S, Filler SA, and Oh CK.** Production of plasminogen activator inhibitor-1 by human mast cells and its possible role in asthma. *J Immunol* 165: 3154–3161, 2000.
13. **Ciano PS, Colvin RB, Dvorak AM, McDonagh J, and Dvorak HF.** Macrophage migration in fibrin gel matrices. *Lab Invest* 54: 62–70, 1986.
14. **Dichtl W, Stiko A, Eriksson P, Goncalves I, Calara F, Banfi C, Ares MP, Hamsten A, and Nilsson J.** Oxidized LDL and lysophosphatidylcholine stimulate plasminogen activator inhibitor-1 expression in vascular smooth muscle cells. *Arterioscler Thromb Vasc Biol* 19: 3025–3032, 1999.
15. **Eddy AA.** Plasminogen activator inhibitor-1 and the kidney. *Am J Physiol Renal Physiol* 283: F209–F220, 2002.
16. **Eitzman DT, McCoy RD, Zheng X, Fay WP, Shen T, Ginsburg D, and Simon RH.** Bleomycin-induced pulmonary fibrosis in transgenic mice that either lack or overexpress the murine plasminogen activator inhibitor-1 gene. *J Clin Invest* 97: 232–237, 1996.
17. **Emeis JJ and Kooistra T.** Interleukin 1 and lipopolysaccharide induce an inhibitor of tissue-type plasminogen activator in vivo and in cultured endothelial cells. *J Exp Med* 163: 1260–1266, 1986.
18. **Fisher L and van Belle G.** *Biostatistics–a methodology for the health sciences.* New York: Wiley, 1993.
19. **George CL, Jin H, Wohlford-Lenane CL, O'Neill ME, Phipps JC, O'Shaughnessy P, Kline JN, Thorne PS, and Schwartz DA.** Endotoxin responsiveness and subchronic grain dust-induced airway disease. *Am J Physiol Lung Cell Mol Physiol* 280: L203–L213, 2001.
20. **Hamelmann E, Schwarze J, Takeda K, Oshiba A, Larsen GL, Irvin CG, and Gelfand EW.** Noninvasive measurement of airway responsiveness in allergic mice using barometric plethysmography. *Am J Respir Crit Care Med* 156: 766–775, 1997.
21. **Hattori N, Degen JL, Sisson TH, Liu H, Moore BB, Pandrangi RG, Simon RH, and Drew AF.** Bleomycin-induced pulmonary fibrosis in fibrinogen-null mice. *J Clin Invest* 106: 1341–1350, 2000.
22. **Kodama M, Naito M, Nomura H, Iguchi A, Thompson WD, Stirk CM, and Smith EB.** Role of D and E domains in the migration of vascular smooth muscle cells into fibrin gels. *Life Sci* 71: 1139–1148, 2002.
23. **Kotani I, Sato A, Hayakawa H, Urano T, Takada Y, and Takada A.** Increased procoagulant and antifibrinolytic activities in the lungs with idiopathic pulmonary fibrosis. *Thromb Res* 77: 493–504, 1995.
24. **Lund LR, Riccio A, Andreasen PA, Nielsen LS, Kristensen P, Laiho M, Saksela O, Blasi F, and Dano K.** Transforming growth factor-beta is a strong and fast acting positive regulator of the level of type-1 plasminogen activator inhibitor mRNA in WI-38 human lung fibroblasts. *EMBO J* 6: 1281–1286, 1987.
25. **Lundblad LK, Irvin CG, Adler A, and Bates JH.** A reevaluation of the validity of unrestrained plethysmography in mice. *J Appl Physiol* 93: 1198–1207, 2002.
26. **Mackarel AJ, Cottell DC, Russell KJ, FitzGerald MX, and O'Connor CM.** Migration of neutrophils across human pulmonary endothelial cells is not blocked by matrix metalloproteinase or serine protease inhibitors. *Am J Respir Cell Mol Biol* 20: 1209–1219, 1999.
27. **Mazzieri R, Masiero L, Zanetta L, Monea S, Onisto M, Garbisa S, and Mignatti P.** Control of type IV collagenase activity by components of the urokinase-plasmin system: a reg-

ulatory mechanism with cell-bound reactants. *EMBO J* 16: 2319–2332, 1997.
28. **Naito M, Stirk CM, Smith EB, and Thompson WD.** Smooth muscle cell outgrowth stimulated by fibrin degradation products. The potential role of fibrin fragment E in restenosis and atherogenesis. *Thromb Res* 98: 165–174, 2000.
29. **Olman MA, Mackman N, Gladson CL, Moser KM, and Loskutoff DJ.** Changes in procoagulant and fibrinolytic gene expression during bleomycin-induced lung injury in the mouse. *J Clin Invest* 96: 1621–1630, 1995.
30. **Ploplis VA, Cornelissen I, Sandoval-Cooper MJ, Weeks L, Noria FA, and Castellino FJ.** Remodeling of the vessel wall after copper-induced injury is highly attenuated in mice with a total deficiency of plasminogen activator inhibitor-1. *Am J Pathol* 158: 107–117, 2001.
31. **Savov JD, Gavett SH, Brass DM, Costa DL, and Schwartz DA.** Neutrophils play a critical role in development of LPS-induced airway disease. *Am J Physiol Lung Cell Mol Physiol* 283: L952–L962, 2002.
32. **Sawdey M, Podor TJ, and Loskutoff DJ.** Regulation of type 1 plasminogen activator inhibitor gene expression in cultured bovine aortic endothelial cells. Induction by transforming growth factor-beta, lipopolysaccharide, and tumor necrosis factor-alpha. *J Biol Chem* 264: 10396–10401, 1989.
33. **Schwartz DA, Thorne PS, Jagielo PJ, White GE, Bleuer SA, and Frees KL.** Endotoxin responsiveness and grain dust-induced inflammation in the lower respiratory tract. *Am J Physiol Lung Cell Mol Physiol* 267: L609–L617, 1994.
34. **Sisson TH, Hanson KE, Subbotina N, Patwardhan A, Hattori N, and Simon RH.** Inducible lung-specific urokinase expression reduces fibrosis and mortality after lung injury in mice. *Am J Physiol Lung Cell Mol Physiol* 283: L1023–L1032, 2002.
35. **Vassalli JD, Sappino AP, and Belin D.** The plasminogen activator/plasmin system. *J Clin Invest* 88: 1067–1072, 1991.
36. **Vu TH and Werb Z.** Matrix metalloproteinases: effectors of development and normal physiology. *Genes Dev* 14: 2123–2133, 2000.
37. **Waltz DA, Natkin LR, Fujita RM, Wei Y, and Chapman HA.** Plasmin and plasminogen activator inhibitor type 1 promote cellular motility by regulating the interaction between the urokinase receptor and vitronectin. *J Clin Invest* 100: 58–67, 1997.
38. **Wilson JW and Li X.** The measurement of reticular basement membrane and submucosal collagen in the asthmatic airway. *Clin Exp Allergy* 27: 363–371, 1997.
39. **Yu Q and Stamenkovic I.** Cell surface-localized matrix metalloproteinase-9 proteolytically activates TGF-beta and promotes tumor invasion and angiogenesis. *Genes Dev* 14: 163–176, 2000.